



## Research Article

# Optimization of ultrasound-assisted extraction of protein from the by-product of the hazelnut oil industry using reverse micelles

Elif Meltem İŞÇİMEN<sup>1,\*</sup> , Mehmet HAYTA<sup>1</sup> 

<sup>1</sup>Department of Food Engineering, Faculty of Engineering, Erciyes University Kayseri, 38280, Türkiye

## ARTICLE INFO

### Article history

Received: 25 January 2023

Revised: 03 March 2023

Accepted: 01 April 2023

### Keywords:

AOT; Hazelnut Waste; FTIR;

Optimization; Ultrasound

## ABSTRACT

In the current research, an ultrasound-assisted extraction (UAE) procedure was established for the protein extracted employing a reverse micelles system (RMS) from the by-product of the hazelnut oil industry. The optimum extraction circumstances in the UAE were identified as a dioctyl sodium sulfosuccinate (AOT) an amount of 0.05 g/mL, a water content of 25.2 ( $W_0$ ), a 0.02 g/mL solid-to-liquid ratio, ultrasound time of 17.52 min, ultrasound cycle 1, and ultrasound power 80% using the response surface approach. Under ideal circumstances, the maximum yield was recorded as 44.84 mg BSA/g of hazelnut meal protein (HMP) for RMS, it had a higher yield obtained by alkaline solution (AS).  $\alpha$ -helix,  $\beta$ -turn, and  $\beta$ -sheet structures of HMP increased while the random coil decreased as evidenced by FTIR and SEM images proving that the cell walls were destructed and had more cracks in RMS. Overall, the findings indicated that UAE combined with RMS might be an effective approach for extracting protein from HMP and is likely to lead to an alternative evaluation possibility of an industrial by-product.

**Cite this article as:** İşçimen EM, Hayta M. Optimization of ultrasound-assisted extraction of protein from the by-product of the hazelnut oil industry using reverse micelles. Sigma J Eng Nat Sci 2024;42(4):1202–1213.

## INTRODUCTION

Extraction from food waste has been increasingly popular as a means of decreasing environmental concerns and resources from waste plants [1]. It is becoming increasingly common to employ hazelnut by-products as natural antioxidants and functional food ingredients [2]. Turkey leads the globe in hazelnut production with 665 TMT in 2020 [3]. Hazelnut meal is produced as a feed ingredient that is obtained following the pressing and extraction of oil

production from hazelnuts. However, it might be used as a nutritional raw material, because of its rich nutritional content [4]. The rheological properties and functional qualities of hazelnut meal products [5], microwave-assisted antioxidant compound extraction from hazelnut [2], edible film-forming potentials of hazelnut meal protein (HMP) obtained after hot extraction, acetone washing, or a combination of methods [6] have been reported. Although there are many investigations on HMP extraction,

### \*Corresponding author.

\*E-mail address: [eliferen@erciyes.edu.tr](mailto:eliferen@erciyes.edu.tr)

*This paper was recommended for publication in revised form by Editor in Chief Ahmet Selim Dalkilic*



ultrasound-assisted extraction (UAE) by the reverse micelles system (RMS) has not been reported.

The UAE has recently gained importance as a method for extracting bioactive from plant materials and increasing extraction efficiency and decreasing extraction time [7]. The matrix is mechanically affected by ultrasound, which causes it to break apart and form smaller particles, giving the extraction fluid more surface area [8]. A study employed UAE with RMS due to the obtained protein from wheat germ [9].

In nonpolar solvents, surfactant molecules aggregate into nanometer-sized aggregates with water molecules as inner cores. RM are biotechnologically essential due to their capacity to saturate their polar cores with water and hydrophilic molecules like proteins [10]. Surfactant-mediated extraction might be used to extract bioactive components such as polyphenols, lectins, and proteins [11-13]. RMS divides protein extraction into two stages: forward and backward extraction. Proteins solubilize into the RMS in the forward extraction process, whereas during the backward extraction phase, the solubilized proteins recover from the RMS [14]. RMS has various benefits over other protein processing methods, including the retention of natural functional characteristics, little interfacial tension, high yield, simplicity of scaling up, and the ability to process continuously [15]. The characteristic properties of protein change with RMS extraction especially the secondary structure of the protein [16, 17]. When compared to proteins obtained in an aqueous buffer, a reduction in the percentage of  $\beta$ -turn whereas a rise in the  $\beta$ -sheet,  $\alpha$ -helix, and random coil proportion have been reported [18].

Therefore, in this research, UAE and RMS were utilized to improve the forward and backward extraction efficiency of HMP. The six-factor (AOT concentration, water content, ratio, ultrasound pulse and power, and time) were evaluated by one-factor analysis before the optimization process. One-factor findings based on ultrasonic power, application time, and the ratio was applied to response surface methodology (RSM). Additionally, the secondary structure and protein content of HMP extracted at its peak using RMS and alkaline solution (AS) were studied. The objective of the current investigation was to employ a novel extraction method that would offer better protein yields and greater activity.

## MATERIALS AND METHODS

### Materials

Diocetyl sodium sulfosuccinate (AOT) (D201170), potassium chloride (KCl) (44675), and isooctane (104727) were bought from Sigma-Aldrich (St. Louis, MO, USA). The substances utilized in the current investigation were of analytical grade. Hazelnut meals were obtained from the oil industry.

### Preparation Of Reverse Micelles System (RMS)

Isooctane, AOT, and KCl phosphate buffer (pH=7.5) were used to prepare RMS. Firstly, AOT was dissolved in the magnetic stirrer at 25°C and the phosphate buffer containing 0.1 M KCl was added according to the molar ratio of water to RM ( $W_0 = [H_2O]/[AOT]$ ) [19].

### One Factor Tests

For UAE with RMS of HMP, there are a few key aspects to consider; AOT concentration,  $W_0$  ratio, ultrasound pulse, power, and application time. Therefore, the AOT concentration of 0.02-0.1 g/mL, water content ( $W_0$ ) of 5-30, the ratio of 0.01-0.1 g/mL, ultrasound pulse of 0.1-1, ultrasound power of 20-100% amplitude, and application time of 5-20 min. were optimized by RSM of Design Expert (Trial Version 7.0.0, Stat-Ease Inc., USA) with one-factor analysis [9,16].

### Ultrasound-Assisted Extraction (UAE) of HMP

HM was added directly to the extraction process in 20 mL of surfactant solvent into the beaker. The probe of the ultrasound device (UP400S, Hielscher, Germany) was submerged center point of the mixture. After the extraction process, for 10 min, the fluid was centrifuged at 4000 g [19]. After centrifugation, the supernatant of the RM phase loaded with HMP of forward extraction was gathered and the equivalent amount of (pH 7.5) aqueous phase KCl in the amount of 1 mol/L was added. The backward extraction procedure was performed in a magnetic stirrer for 1 h at 25 °C. The protein-rich phase was gathered after centrifugation (4000g,10 min). The Bradford technique was used to determine the protein concentration of the HM extract [20]. A standard curve was established using the BSA.

### Optimization by Response Surface Methodology (RSM)

The surfactant ratio,  $W_0$ , and ultrasound pulse were selected according to a one-factor experiment for further Box-Behnken design (BBD) of RSM of Design-Expert software. The solid-to-liquid ratio, ultrasonic power, and application duration were all optimized to perfection. The findings of the preliminary studies were used to define these optimal ranges, which included application time ( $X_1$ ) 10-20 min., ratio ( $X_2$ ) 0.02-0.06 g/mL, and ultrasound power ( $X_3$ ) 40-80 % amplitude. The protein content of the forward extract was used response factor. In the design, five central points were chosen. As a result, extraction was carried out at a total of seventeen separate points (Table 1). Samples were prepared as 20 mL in beakers with a capacity of 100 mL. After UAE, centrifugation at 4000 g for 10 min separated the undissolved residue, and the content of protein in the supernatant was assessed using the Bradford test.

The suitability and fitness of the model were assessed using ANOVA. Based on the results of the RSM optimization inquiry, the impacts of quadratic effects were

determined using a second-order polynomial model [21].

### Backward Extraction of HMP

The supernatant of the RM phase from the forward extraction that was loaded with HMP was collected, and an equivalent volume of the (pH 7.5) aqueous phase with 1 mol L<sup>-1</sup> of KCl was introduced. The backward transport method was carried out for one hour at 25°C in a magnetic stirrer. Following centrifugation of the mixture (4000 g, 10 min) [22]. The protein-rich solution was collected and the protein was precipitated with the ternary liquid system at 25°C. Acetone, deionized water, and isooctane were combined in a ternary liquid system with a volume ratio of 15:5:1. To eliminate any remaining surfactant, the HMP precipitate was washed with a 65% ethanol solution [23]. Finally, the HMP underwent freeze-drying (Christ Alpha, 1 2 LD plus, Germany), and stored at -20°C.

### Alkaline Extraction

The alkaline solution (AS) (pH 12.0) was used for conventional extraction [21]. The protein was extracted using optimal extraction conditions that had been determined by BBD. A ternary liquid system was then used to precipitate the protein in the supernatant after the mixture had been centrifuged at 4000 g for 10 min. The HMP was freeze-dried in a lyophilizer (Christ Alpha, 1 2 LD plus, Germany) and stored at -20°C for further analysis [16].

### Scanning Electron Microscopy (SEM)

The microstructure properties of lyophilized HMP obtained by UA-RMS and UA-AS were investigated by an SEM (Leica 231 LEO: S-440, Cambridge, USA). A thin gold coating was applied to the HMP. A 25 kV excitation voltage was used for visualization.

### Fourier Transform Infrared (FTIR) Spectroscopy

The secondary structure of HMP samples was determined by FTIR spectroscopy (Spectrum 400, PerkinElmer Instruments, Waltham, USA). ATR unit was used with 4 cm<sup>-1</sup> resolutions. The measurements were made using a 100 scan speed in the wavenumber range of 450-4000 cm<sup>-1</sup>.

### X-Ray Diffraction (XRD)

A diffractometer (D8 Advanced, Bruker AXS GmbH, Karlsruhe, Germany) was used for the analysis. 45 kV and 40 mA were chosen as the voltage and current, respectively. Cu-K nickel was used to filter the radiation, and the wavelength was 1.5406. The scanning speed was 5°/min. Diffraction data were gathered in the 2θ range of 5° to 70° [24].

### Statistical Analysis

Design Expert (Trial Version 7, Stat-Ease Inc., Minneapolis, MN) was used for the optimization process. The suitability of the model was evaluated using the coefficient of determination (R<sup>2</sup>) of ANOVA, lack of fit-derived parameters, and the F-test.

**Table 1.** Protein extraction from hazelnut by-products using the Box-Behnken Design by UAE-RMS

Run	Time (min.) (X1)	Solid/liquid (g/mL) (X2)	Power (amplitude %) (X3)	Protein (mg BSA/g)
1	15.00	0.02	40.00	30.78
2	15.00	0.04	60.00	22.14
3	20.00	0.04	80.00	20.33
4	15.00	0.04	60.00	16.28
5	10.00	0.04	80.00	18.39
6	10.00	0.06	60.00	10.98
7	15.00	0.04	60.00	18.92
8	10.00	0.04	40.00	17.84
9	20.00	0.06	60.00	10.83
10	20.00	0.04	40.00	14.61
11	20.00	0.02	60.00	33.53
12	15.00	0.06	80.00	11.37
13	15.00	0.02	80.00	46.14
14	15.00	0.04	60.00	17.34
15	15.00	0.06	40.00	14.42
16	15.00	0.04	60.00	15.97
17	10.00	0.02	60.00	30.66

## RESULTS AND DISCUSSION

### Optimization of Ultrasound-Assisted Reverse Micelle by One Factor

The water content and AOT concentration are significant parameters affecting HMP yield. Firstly, the AOT concentration was optimized by one-factor analysis under the following condition:  $W_0$  20, ultrasound power 50%, time 10 min., ratio 0.03 g/mL, ultrasound cycle 1. The most effective AOT concentration was found at 0.05 g/mL according to Figure 1a. The HMP yield was increased with an increasing AOT ratio at 0.06 g/mL however, it decreased after 0.06 g/mL. Similarly, in a study, AOT concentration which ranged from 0.04 to 0.08g/mL was optimized for protein extraction from wheat germ. Protein content increased quickly as concentration went from 0.02 to 0.06 g/mL. and as the concentration of AOT rose, the efficiency of forward extraction began to decrease. [19]. These findings concurred with the in another investigation [25]. A faster protein extraction yield of watermelon seed was reported when surfactant concentrations changed from 0.04 to 0.10 mol/L. However, protein yields insignificantly increased after 0.10 mol/L AOT [16].

Subsequently, different water ratios ( $W_0$ : 5-30) have been optimized by keeping the AOT ratio at optimum. It was seen the optimum water content was found as 25.2 (Figure 1b). Firstly, the increase in RMS water content increased HMP yield. The increments of protein yields were insignificant after then 25  $W_0$ . High surfactant concentrations and water content have been demonstrated to enhance the number of surfactant aggregations and modify the surfactant size, hence improving protein transfer into RMS [26]. The optimum  $W_0$  was reported as 20 for protein extraction from watermelon seed [16] and 25 from the wheat germ [19]. The increase in  $W_0$  correlated with an increase in micelle size, and the micelle size highly influenced protein solubilization. The capacity of a protein micelle to be solubilized depended critically on its size. [27]. Larger RM was generated when  $W_0$  was increased, allowing for the inclusion of several protein molecules [28].

The ultrasound power was between 20% and 100% amplitude. The other factor was selected as the concentration of AOT 0.05 g/mL,  $W_0$  25.2, time 10 min., ratio 0.03 g/mL, ultrasound cycle 1. The HMP yield was increased with increasing power up to 80% amplitude. The optimum power was selected as 65.9 % amplitude according to a one-factor design (Figure 1c). Higher protein content at higher ultrasonic amplitudes might be related to structural cell damage caused by ultrasound [29]. However, it has been reported that the power set above 363 W, and the efficiency of UAE did not improve significantly [30]. The application time ranged from 5 to 20 min (Figure 1c). The optimum HMP extraction time was determined as 15.4 min. and the cycle was selected 1 according to Figure 1d.

The ratio was an optimized one-factor test in the present study as a crucial independent variable that affects the dissolving balance of the sample. The effects of the ratio were investigated in the following conditions: concentration of AOT 0.05 g/mL,  $W_0$  25.2, time 10 min., power 65.9%, and ultrasound cycle 1. According to Figure 1e, in the RMS, HMP dissolution approached equilibrium when the ratio was 0.02 g/mL. As a result, The ideal operating of the surfactant process by UAE was found to be 0.02 g/mL. A similar result was reported for protein extraction from watermelon seeds [16].

### Optimization of UAE-RMS

Three parameters; time ( $X_1$ ) solid to liquid ratio ( $X_2$ ), and power ( $X_3$ ) were enhanced via the BBD of RSM. The RSM is a popular method for determining parameters and analyzing response factors [31]. The experimental settings and relevant response levels based on the experimental plan are listed in Table 1. For the recovery of protein from HM, the quadratic model was proposed by the model. The following quadratic regression model illustrates the connection between these factors and overall HMP extraction yields.

$$\text{HMP} = 18.13 + 0.18X_1 - 11.69X_2 + 2.32X_3 - 0.75X_1X_2 + 1.29X_1X_3 - 4.60X_2X_3 - 2.26X_1^2 + 5.63X_2^2 + 1.92X_3^2$$

The ideal HMP extraction parameters were found to be 17.52 min, 0.02 g/mL, and 80% amplitude. As the determined predicted protein yield by RSM was 44.84 mg BSA/g. The model worked well because there wasn't a big gap between experimental and projected values.

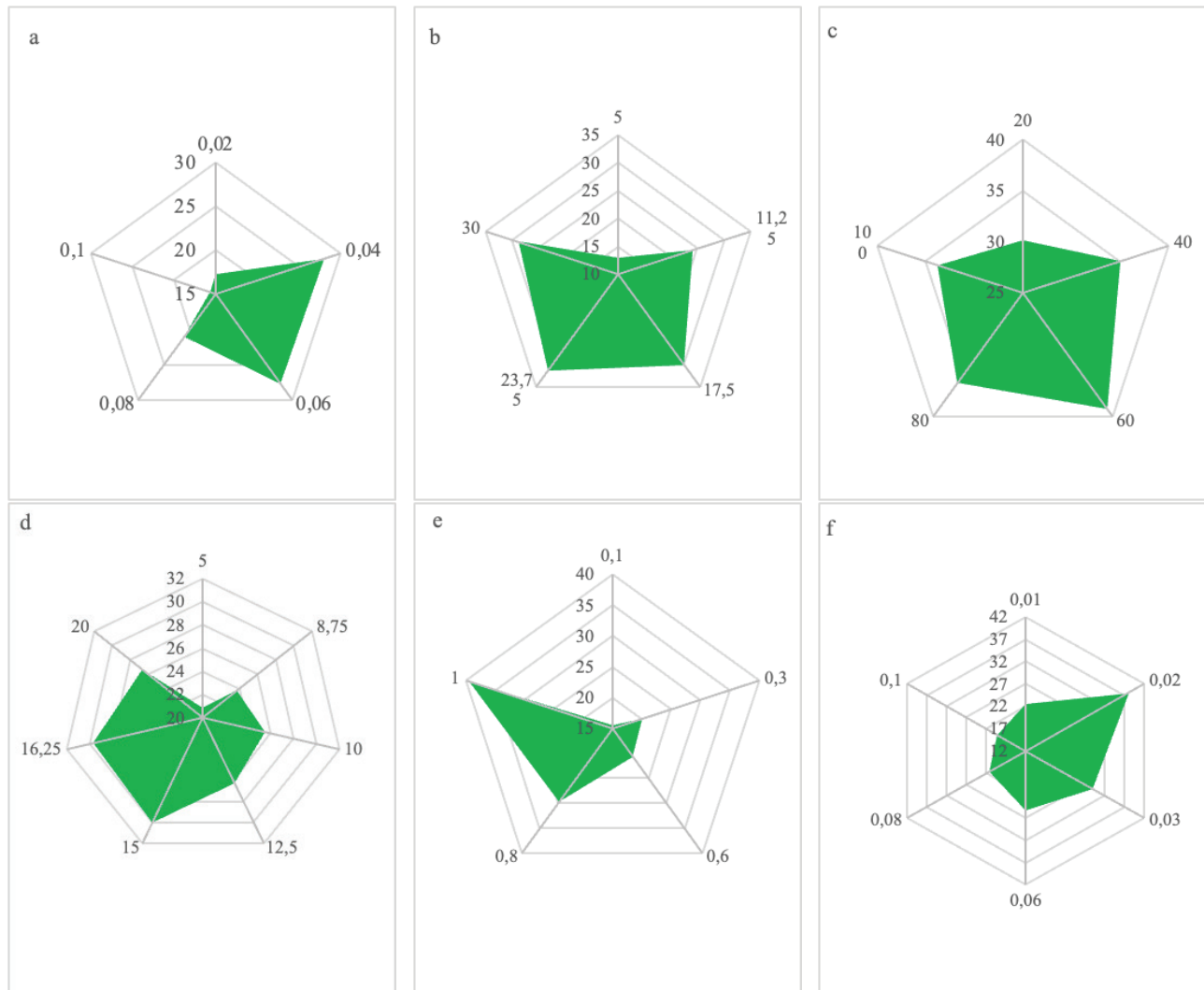
Using the p-value, the statistical significance of the interaction of independent variables was evaluated. The significance and suitability of the quadratic model were assessed using ANOVA data and the results of the ANOVA were shown in Table 2. While the p-values of a model, solid-to-liquid ratio, and power were found as <0.05, time had a p-value greater than 0.05. The lack of fit test, which determines if models are relevant to entirely predict variance, was used to verify the validity of models [32]. The lack of fit value of the model was determined insignificant as >0.05. The determination coefficients ( $R^2$ ) value, adj.  $R^2$  value and pred. The  $R^2$  value of the sample was 0.97, 0.93, and 0.79, respectively. The optimization model of BBD for HMP extraction by UAE-RMS was statistically significant and the experimental data were appropriately fitted by the model.

Figure 2 depicts the interaction of the variables as well as the impact of independent variables on response. The 3-D plot in Figure 2a demonstrated that as ultrasonic power increased, so did the yield of protein extraction. However, the increasing time does not significantly affect extraction yield. The extraction yield suffered as the ratio increased (Figure 2b). Similarly, the ratio showed a similar trend (Figure 2c).

## COMPARISON: UAE-RMS AND UAE-AS AND KINETICS

The best-operating conditions for one factor were: AOT concentration, 0.05 g/mL;  $W_0$ , 25.2; ultrasound cycle, 1.

According to the optimization process of BBD, the ratio is 0.02 g/mL; ultrasound power is 80% amplitude; and time is 17.52 min. UAE- RMS was used to extract the protein under ideal circumstances and the protein obtained UAE-AS at 0.02 g/mL; ultrasound power, 80% amplitude; time, 17.52



**Figure 1.** The one-factor test of ultrasound-assisted extraction (UAE)-reverse micellar solution (RMS).

The impact of AOT ratio on protein production (a); the effect of water ( $W_0$ ) on protein production (b); the effect of ultrasound power on protein production (c); the effect of time on protein production (d); the effect of ultrasound cycle on protein production (e); the impact of the solids-to-liquids ratio on protein production (f).

One Factor	p-value				
	Model	Lack of fit	Independent variable	Point prediction	$R^2$
AOT (g/ mL)	0.00	0.41	0.01	0.05	0.99
$W_0$	0.00	0.99	0.00	25.2	0.96
Power (% Amplitude)	0.01	0.38	0.04	65.9	0.91
Time (min)	0.01	0.24	0.00	15.4	0.93
Cycle	0.00	0.10	0.00	1.00	0.98
Solid/liquid (g/mL)	0.00	0.42	0.00	0.02	0.10

**Table 2.** ANOVA for the recovery of protein from the by-product of hazelnut

	Sum of squares	DF	Mean square	F-value
Model	1398.54	9	155.39	26.18****
X <sub>1</sub> : Time (min)	0.25	1	0.25	0.043ns
X <sub>2</sub> : Solid/liquid (g/mL)	1092.87	1	1092.87	184.12****
X <sub>3</sub> :Power (% amplitude)	43.17	1	43.17	7.27*
X <sub>1</sub> X <sub>2</sub>	2.27	1	2.27	0.38ns
X <sub>1</sub> X <sub>3</sub>	6.67	1	6.67	1.12ns
X <sub>2</sub> X <sub>3</sub>	84.81	1	84.81	14.29**
X <sub>1</sub> <sup>2</sup>	21.49	1	21.49	3.62ns
X <sub>2</sub> <sup>2</sup>	133.43	1	133.43	22.48**
X <sub>3</sub> <sup>2</sup>	15.52	1	15.52	2.61ns
Residual	41.55	7	5.94	
Lack of fit	16.14	3	5.38	0.85ns
Pure error	25.41	4	6.35	
Core total	1440.09	16		
R-Squared 0.97				
Adj R-Squared 0.93				
Pred R-Squared 0.79				
Adeq Precision 18.76				

\*p≤ 0.05; \*\*p≤ 0.01; \*\*\*p≤ 0.001; \*\*\*\*p≤ 0.0001; ns p>0.05

min. When the extraction yield was compared, it was seen that the RMS was more effective than AS. The protein content was found for RMS and AS as 53.58±0.4 and 22.62±1.00 mg BSA/g, respectively. The variation of protein yield over time for both systems was given in Figure 3. The second-order kinetic model (Eq. 1) was used to evaluate the extraction's kinetics [33]. Moreover, the initial extraction rate is specified by Eq. 2 as time t approaches zero and the root means square error (RMSE) was determined according to Eq. 3 using the Statistica (Tibco Software Inc. USA).

$$CL(t) = \frac{Ce^2kt}{1+Ce^2kt} = \frac{Cet}{\left(\frac{1}{Cek}\right)+t} \quad (1)$$

$$h = kCe^2 \quad (2)$$

$$RMSE = \sqrt{\sum_{i=1}^n \frac{[CL,p(t)-CL,e(t)]^2}{n}} \quad (3)$$

Time, t (min), second-order release rate constant, k (g mg<sup>-1</sup> min<sup>-1</sup>), initial releasing rate, h (mg g<sup>-1</sup> min<sup>-1</sup>), the concentration of protein, Ce (mg/g), CL, p model-predicted protein content (mg L<sup>-1</sup>) CL, e protein content obtained experimentally (mg L<sup>-1</sup>).

The h and k value was found as 54.15 mg g<sup>-1</sup> min<sup>-1</sup> and 0.024 g mg<sup>-1</sup> min<sup>-1</sup> for RMS, respectively, and higher than AS. This verified that the UAE-RMS could greatly improve

the extraction rates of protein from HM. A similar study reported that the RM extraction of AOT-SDS/isooctane was an efficient and successful method for separating full-fat peanut powder sources of peanut protein [34]. In addition, researchers have examined the dynamics of protein partitioning for batch protein extraction using RM phases containing AOT in isooctane [10]. In another comparison study, the protein yield of the RMS was found more effective than the AS [16].

#### SEM Analysis of HMP

Figure 4 shows the SEM micro-images of HMP after UAE-RMS (Figure 4 a, b) and alkaline extraction (Figure 4 c, d). The cell structure of the HMP extracted by AS was more intact and smooth according to the HMP extract obtained from RMS. This finding suggested that the ultrasound application with RMS might cause cell walls to be destroyed. The cell walls were destructed and had more cracks in RMS. A similar result was reported for a watermelon seed protein extraction [16]. Literature suggested that the RM approach might alter walnut microstructure [24]. Similarly, a study reported that peanut proteins obtained by RMS had more holes on their surfaces, which were made up of a discontinuous and loose network according to proteins abtained by the aqueous buffer [24]. When the persistent network transitions to the discontinuous phase, RM may produce hydrophobic interactions, electrostatic contacts, and, hydrogen bonds acting as a junction zone and providing additional structural support [35]. It has been known that protein microstructure might

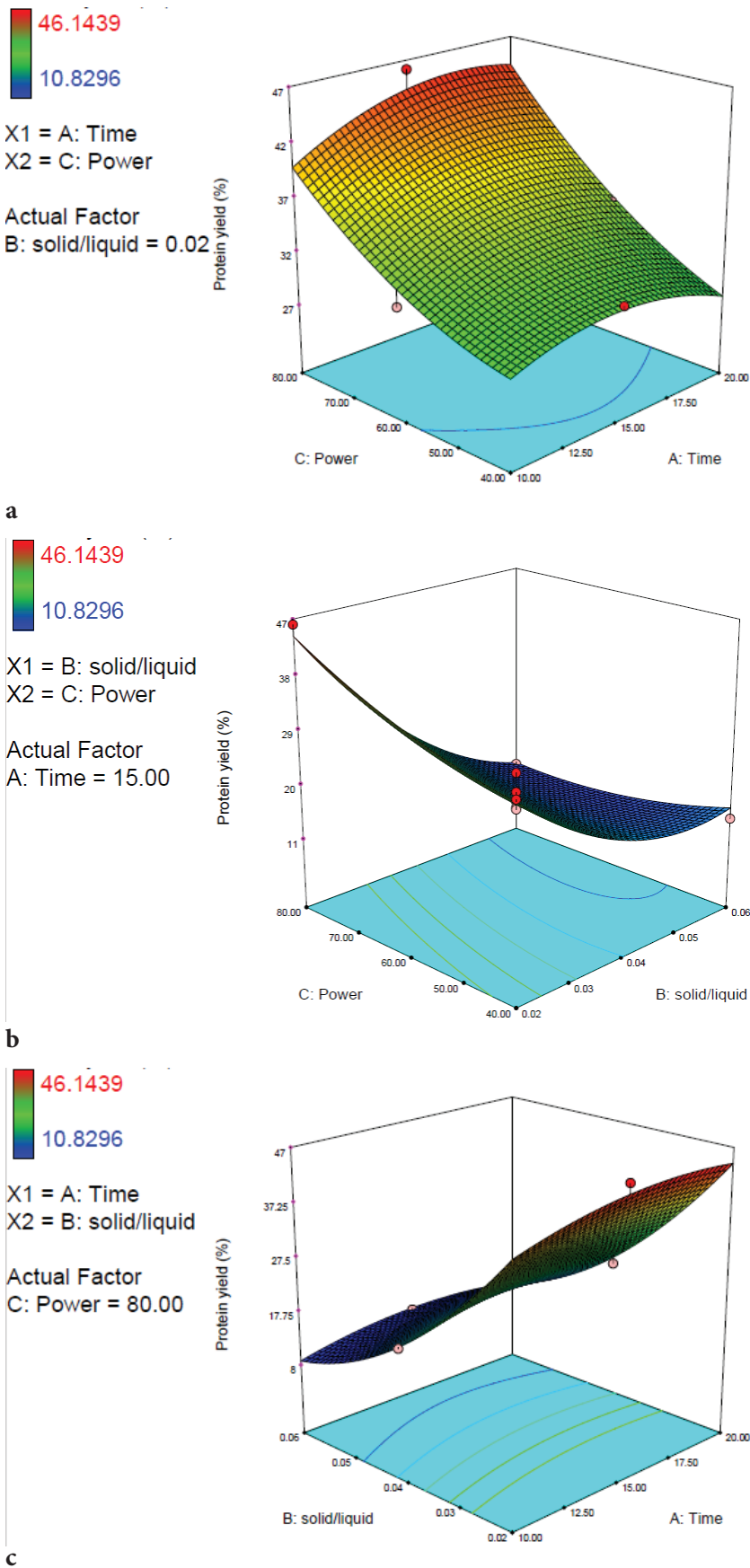
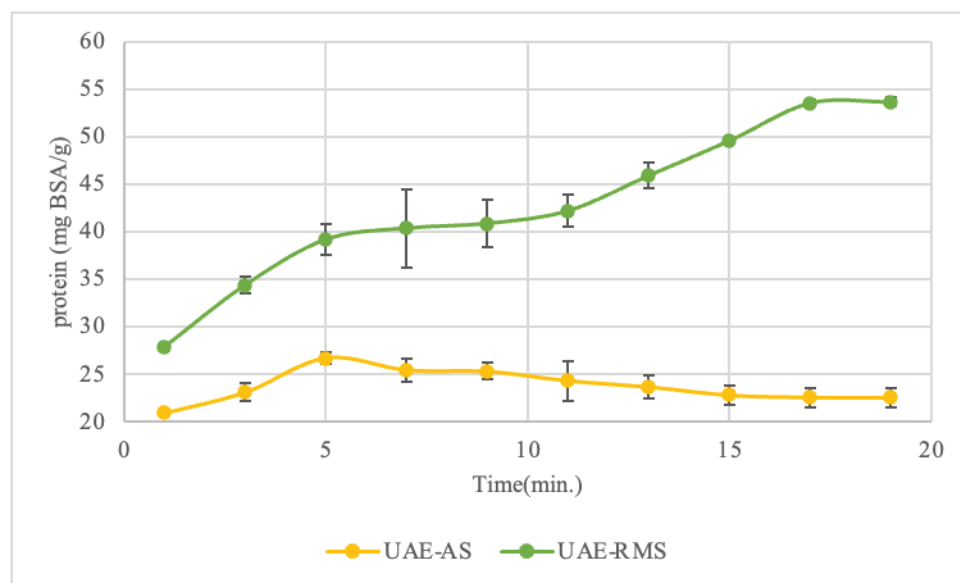


Figure 2. 3D plots optimization by Box Behnken Design (BBD)



	h	k	Ce	RMSE
UAE-RMS	54.15	0.024	47.50	3.62
UAE-AS	40.03	0.015	51.66	1.36

**Figure 3.** The comparative study and kinetics of ultrasound-assisted extraction-reverse micelles system (UAE-RMS) and ultrasound-assisted extraction-alkaline system (UAE-AS).

h: initial releasing rate ( $\text{mg g}^{-1} \text{min}^{-1}$ ); k: second-order release rate constant ( $\text{g mg}^{-1} \text{min}^{-1}$ ); Ce: concentration of protein ( $\text{mg/g}$ ), RMSE: root mean square error ( $\text{mg/g}$ ).

influence the physicochemical properties leading to alterations in and functional performance of proteins [36, 37].

### FTIR Spectroscopy

The FTIR approach is effective in determining the secondary structure of the protein. The functional groups in the two proteins were identified using FTIR spectra in the  $400\text{--}4000 \text{ cm}^{-1}$  range. (Figure 5 a). RMS and AS were used to quantify the secondary structure of proteins that the UAE had retrieved, and the data from curve fitting was standardized for the amide I region. ( $1700\text{--}1600 \text{ cm}^{-1}$ ) (Figure 5 b,c). The amide I band was superimposed using a Gaussian curve fitting approach by Origin, and the results showed that the detection method was suitable. The compositions of HMP secondary structures were also shown in Table 3.

The four main parts of the protein secondary structure are  $\alpha$ -helix,  $\beta$ -sheet,  $\beta$ -turn, and random coil structures. The internal structure of a protein which is  $\alpha$ -helix and  $\beta$ -sheet is determined by intermolecular hydrogen bonds, which indicates the protein's high order. The flexibility of protein is linked to the random coil [16]. For the  $\alpha$ -helix structure, bands between  $1650\text{--}1663 \text{ cm}^{-1}$  were used. The region of the  $\beta$ -sheet was determined according to bands  $1612\text{--}1640 \text{ cm}^{-1}$ ,  $1670\text{--}1694 \text{ cm}^{-1}$ . When the  $\beta$ -turn was investigated according to  $1664\text{--}1684 \text{ cm}^{-1}$ ,  $1694\text{--}1696$

$\text{cm}^{-1}$ , the random coil was determined as stated by  $1640\text{--}1650 \text{ cm}^{-1}$  [24, 38]. In Figure 3a, it was seen that the sharp peak was observed between  $1612\text{--}1640 \text{ cm}^{-1}$ . However, the peak of UAE-AS was weaker than UAE-RMS. These results indicated that a higher  $\beta$ -sheet structure of HMP was obtained via RMS.

When RMS was utilized as a solvent, the quantity of  $\alpha$ -helix,  $\beta$ -sheet, and  $\beta$ -turn structure increased and the amount of random coil structure decreased (Table 3). The  $\alpha$ -helix,  $\beta$ -sheet, and  $\beta$ -turn structure may convert into a random coil shape due to the varying microenvironment for protein extraction [39]. The increase in random coil structure might be due to protein denaturation/unfolding after standard AS extraction [40–42]. In the present study, Variable degrees of random coil structures were introduced into the  $\beta$ -sheet,  $\alpha$ -helix, and  $\beta$ -turn structures., implying that HMP was denatured by alkaline extraction. Similar to the current study, an increase in the  $\alpha$ -helix and  $\beta$ -turn structures in RMS was reported. Watermelon seed protein found an increase in the  $\beta$ -sheet and  $\beta$ -turn in RMS, and a decrease in the  $\alpha$ -helix structure [16]. The findings of the current study suggest that the protein function or activity of HMP extracted by UAE-RMS maintains, however in various microenvironment settings, and the secondary structure compositions of HMP fractions might alter.

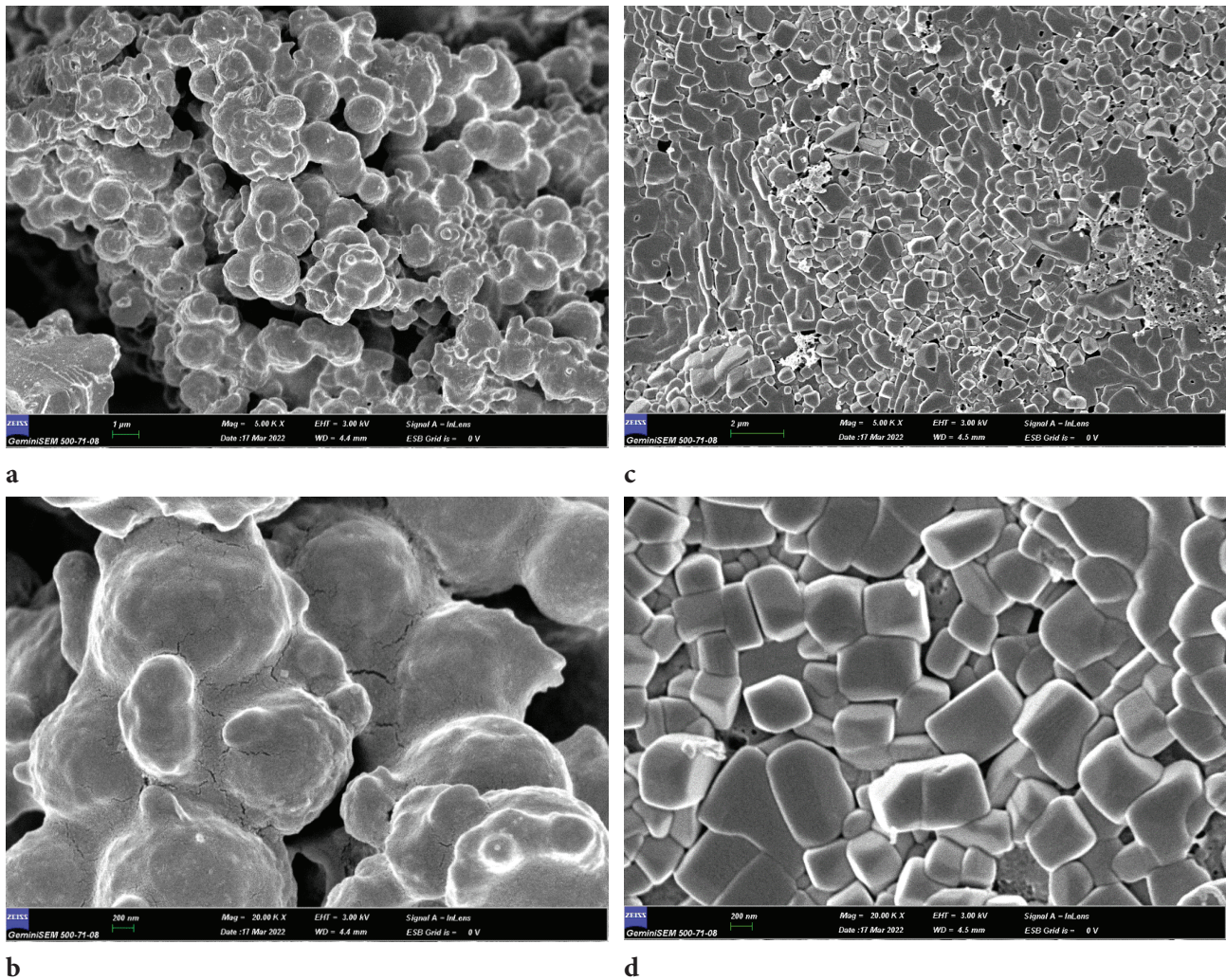


**Figure 4.** Scanning electron microscopy (SEM) spectra hazelnut meal protein (HMP) obtained by ultrasound-assisted extraction (UAE)-reverse micellar solution (RMS) (a,b); UAE-alkaline solution (AS) (c,d).

**Table 3.** FTIR analysis

	$\alpha$ -helix (%) (1650-1663 $\text{cm}^{-1}$ )	$\beta$ -Sheet (%) (1670-1694 $\text{cm}^{-1}$ 1612-1640 $\text{cm}^{-1}$ )	$\beta$ -turn (%) (1694-1696 $\text{cm}^{-1}$ 1664-1684 $\text{cm}^{-1}$ )	Random coil (%) (1640-1650 $\text{cm}^{-1}$ )
UAE-RMS	14.74	31.66	21.45	32.13
UAE-AS	7.28	27.2	17.3	48.21

UAE-RMS: Ultrasound assisted extraction- reverse micelles system.

UAE-AS: Ultrasound-assisted extraction- alkaline solution.

## XRD

The use of XRD patterns to determine the crystallinity of inorganic polymer materials is a useful approach [43]. Figure 6 shows the XRD pattern of HMP extracted by UAE-RMS and UAE-AS. The overall spectra shape is much similar to HMP obtained with UAE-RMS and UA-AS. A significant crystalline peak was visible in the HMP recovered using AS

and RMS, with a 2 value between  $28.40^\circ$  and  $40.50^\circ$ . The peak of UAE-AS was higher than the peak of UAE-RMS. Furthermore, the intensity of a peak might show changes in the structure of the protein [24]. The findings revealed that the backbone structures of HMP are almost identical. The tiny peaks were observed at a  $2\theta$  value of about  $50.30^\circ$ ,  $58.70^\circ$ , and  $66.50^\circ$ . When pure HMP failed to show

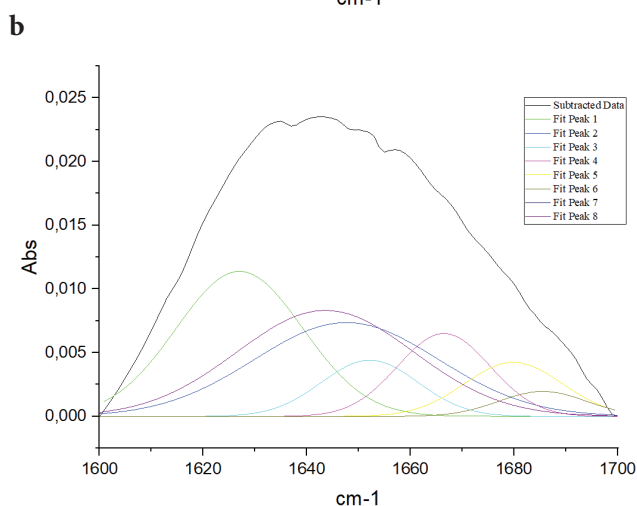
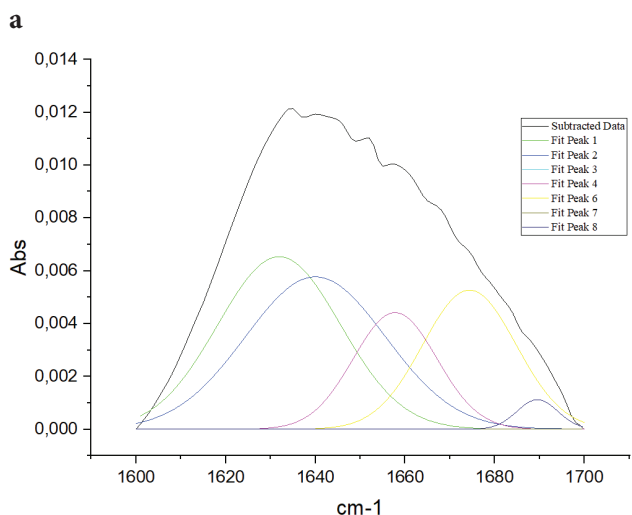
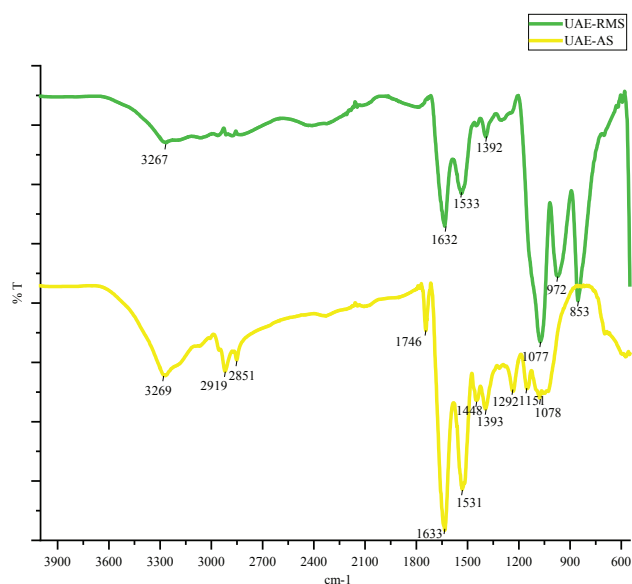


**Figure 5.** Fourier transform infrared (FTIR) spectra HMP extracted by UAE-RMS and UAE-AS (a); The curve-fitting amide I band spectra (1700–1600  $\text{cm}^{-1}$ ) of hazelnut meal protein (HMP) obtained by ultrasound-assisted extraction (UAE)-reverse micellar solution (RMS) (b); UAE-alkaline solution (AS) (c).

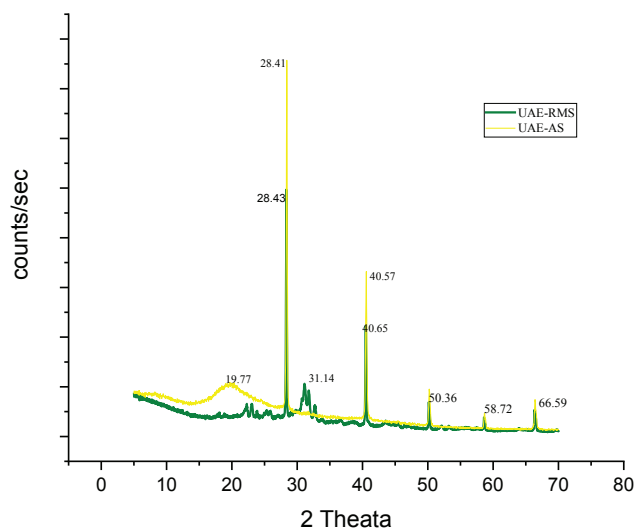


**Figure 6.** X-ray diffraction (XRD) spectra.

UAE-RMS: ultrasound-assisted extraction- reverse micellar solution

UAE-AS: ultrasound-assisted extraction-alkaline solution

any discernible intensity peaks in the XRD diffraction pattern spectrum, the presence of gold nanoparticles could be detected in the visible range of the spectrophotometer [43]. The results of this investigation are consistent with previous research [37, 44].

## CONCLUSION

In the present work, the utilization of AOT-RMS which is a new technique to obtain HMP was successfully performed in this study. Throughout the UAE, RMS effectively damaged the hazelnut meal cells. Because the hydrogen bonds and electrostatic and hydrophobic interactions of the RMS aggregates facilitated the transport of HMP into RMS. In addition, since surfactant and organic solvent recycling were ecologically benign, protein is obtained by an environmentally friendly method. The optimization study was conducted due to determine the most effective extraction parameters. Firstly, one-factor analysis has been applied to set optimization limits. According to a one-factor analysis, BBD was applied. The protein isolate was produced at the optimum point for UAE-RMS. In order to test the effectiveness of RMS, the protein was produced at optimum points by using AS instead of RMS. In a comparative study, it was found that the UAE-RMS had greater extraction yields than the UAE-AS. The evaluation of the secondary structure of protein revealed that  $\alpha$ -helix,  $\beta$ -turn, and  $\beta$ -sheet structures of HMP obtained by UAE-RMS were 14.74%, 31.66%, and 21.45%, respectively while the  $\alpha$ -helix,  $\beta$ -turn, and  $\beta$ -sheet structure of HMP obtained by UAE-AS were 7.28%, 27.2%, and 17.3%, interpreted as changing the functional properties of the protein. UAE-RMS proved very

useful in obtaining HMP indicating a potential for scaling up the RMS and UAE approach into a commercial process. However, to ascertain the effect of UAE-RMS on the technologically useful features of HMP, more investigation is required.

## AUTHORSHIP CONTRIBUTIONS

Authors equally contributed to this work.

## DATA AVAILABILITY STATEMENT

The authors confirm that the data that supports the findings of this study are available within the article. Raw data that support the finding of this study are available from the corresponding author, upon reasonable request.

## CONFLICT OF INTEREST

The author declared no potential conflicts of interest with respect to the research, authorship, and/or publication of this article.

## ETHICS

There are no ethical issues with the publication of this manuscript.

## REFERENCES

- [1] El-Adawy TA, Taha KM. Characteristics and composition of watermelon, pumpkin, and paprika seed oils and flours. *J Agric Food Chem* 2001;49:1253-1259. [\[CrossRef\]](#)
- [2] Bener M, Şen FB, Önem AN, Bekdeşer B, Çelik SE, Lalikoglu M, et al. Microwave-assisted extraction of antioxidant compounds from by-products of Turkish hazelnut (*Corylus avellana* L.) using natural deep eutectic solvents: Modeling, optimization and phenolic characterization. *Food Chem* 2022;385:132633. [\[CrossRef\]](#)
- [3] FAOSTAT. 2020: <https://www.fao.org/faostat/en/#data/QCL/visualize>.
- [4] Sen D, Kahveci D. Production of a protein concentrate from Hazelnut meal obtained as a hazelnut oil industry by-product and its application in a functional beverage. *Waste Biomass Valori* 2020;11:5099-5107. [\[CrossRef\]](#)
- [5] Tatar F, Tunç MT, Kahyaoglu T. Turkish Tömbül hazelnut (*Corylus avellana* L.) protein concentrates: Functional and rheological properties. *J Food Sci Technol* 2015;52:1024-1031. [\[CrossRef\]](#)
- [6] Aydemir LY, Gökbulut AA, Baran Y, Yemencioğlu A. Bioactive, functional and edible film-forming properties of isolated hazelnut (*Corylus avellana* L.) meal proteins. *Food Hydrocoll* 2014;36:130-142. [\[CrossRef\]](#)
- [7] Kumar K, Srivastav S, Sharanagat VS. Ultrasound assisted extraction (UAE) of bioactive compounds from fruit and vegetable processing by-products: A review. *Ultrason Sonochem* 2021;70:105325. [\[CrossRef\]](#)
- [8] Rostagno MA, Palma M, Barroso CG. Ultrasound-assisted extraction of soy isoflavones. *J Chromatogr A* 2003;1012:119-128. [\[CrossRef\]](#)
- [9] Zhu KX, Sun XH, Zhou HM. Optimization of ultrasound-assisted extraction of defatted wheat germ proteins by reverse micelles. *J Cereal Sci* 2009;50:266-271. [\[CrossRef\]](#)
- [10] Lye GJ, Asenjo JA, Pyle DL. Protein extraction using reverse micelles: kinetics of protein partitioning. *Chem Eng Sci* 1994;49:3195-3204. [\[CrossRef\]](#)
- [11] He S, Shi J, Walid E, Ma Y, Xue SJ. Extraction and purification of a lectin from small black kidney bean (*Phaseolus vulgaris*) using a reversed micellar system. *Process Biochem* 2013;48:746-752. [\[CrossRef\]](#)
- [12] Liu F, Wang X, Zhao X, Hu H, Chen F, Sun Y. Surface properties of walnut protein from AOT reverse micelles. *Int J Food Sci Technol* 2014;49:626-633. [\[CrossRef\]](#)
- [13] Li F, Raza A, Wang YW, Xu XQ, Chen GH. Optimization of surfactant-mediated, ultrasonic-assisted extraction of antioxidant polyphenols from rattan tea (*Ampelopsis grossedentata*) using response surface methodology. *Pharmacogn Mag* 2017;13:446-453. [\[CrossRef\]](#)
- [14] Leser ME, Mrkoci K, Luisi PL. Reverse micelles in protein separation: the use of silica for the back-transfer process. *Biotechnol Bioeng* 1993;41:489-492. [\[CrossRef\]](#)
- [15] Chuo SC, Mohd-Setapar SH, Mohamad-Aziz SN, Starov VM. A new method of extraction of amoxicillin using mixed reverse micelles. *Colloids Surf A Physicochem Eng Asp* 2014;460:137-144. [\[CrossRef\]](#)
- [16] Liu L, Xi J. Mechanochemical-assisted extraction of protein from watermelon seeds with surfactant. *LWT* 2021;142:111025. [\[CrossRef\]](#)
- [17] Naoe K, Noda K, Kawagoe M, Imai M. Higher order structure of proteins solubilized in AOT reverse micelles. *Colloids Surf B Biointerfaces* 2004;38:179-185. [\[CrossRef\]](#)
- [18] Chen X, Ru Y, Chen F, Wang X, Zhao X, Ao Q. FTIR spectroscopic characterization of soy proteins obtained through AOT reverse micelles. *Food Hydrocoll* 2013;31:435-437. [\[CrossRef\]](#)
- [19] Sun XH, Zhu KX, Zhou HM. Protein extraction from defatted wheat germ by reverse micelles: Optimization of the forward extraction. *J Cereal Sci* 2008;48:829-835. [\[CrossRef\]](#)
- [20] Bradford MM. A rapid and sensitive method for the quantitation of microgram quantities of protein utilizing the principle of protein-dye binding. *Anal Biochem* 1976;72:248-254. [\[CrossRef\]](#)

- [21] Wani AA, Sogi DS, Grover L, Saxena DC. Effect of temperature, alkali concentration, mixing time and meal/solvent ratio on the extraction of watermelon seed proteins - A response surface approach. *Biosyst Eng* 2006;94:67-73. [\[CrossRef\]](#)
- [22] Chen J, Chen F, Wang X, Zhao X, Ao Q. The forward and backward transport processes in the AOT/hexane reversed micellar extraction of soybean protein. *J Food Sci Technol* 2014;51:2851-2856.
- [23] Sun XH, Zhu KX, Zhou HM. Optimization of a novel backward extraction of defatted wheat germ protein from reverse micelles. *Innov Food Sci Emerg Technol* 2009;10:328-333. [\[CrossRef\]](#)
- [24] Zhao X, Liu H, Zhang X, Zhu H, Ao Q. Surface structure and volatile characteristic of peanut proteins obtained through AOT reverse micelles. *Colloids Surf B Biointerfaces* 2019;173:860-868. [\[CrossRef\]](#)
- [25] Lye GJ, Asenjo JA, Pyle DL. Extraction of lysozyme and ribonuclease-a using reverse micelles: Limits to protein solubilization. *Biotechnol Bioeng* 1995;47:509-519. [\[CrossRef\]](#)
- [26] Wolbert RB, Hilhorst R, Voskuilen G, Nachtegaal H, Dekker M, Riet KVT, et al. Protein transfer from an aqueous phase into reversed micelles. *Eur J Biochem* 1989;184:627-633. [\[CrossRef\]](#)
- [27] Cöklen KE, Hatton TA. Protein extraction using reverse micelles. *Biotechnol Progress* 1985;1:69-74. [\[CrossRef\]](#)
- [28] Ichikawa S, Imai M, Shimizu M. Solubilizing water involved in protein extraction using reversed micelles. *Biotechnol Bioeng* 1992;39:20-26. [\[CrossRef\]](#)
- [29] Geow CH, Tan MC, Yeap SP, Chin NL. Application of osmotic dehydration and ultrasound to enhance hazelnut oil extraction. *Food Anal Methods* 2021;14:411-421. [\[CrossRef\]](#)
- [30] Wei F, Gao GZ, Wang XF, Dong XY, Li PP, Hua W, et al. Quantitative determination of oil content in small quantity of oilseed rape by ultrasound-assisted extraction combined with gas chromatography. *Ultrason Sonochem* 2008;15:938-942. [\[CrossRef\]](#)
- [31] Xu Y, Zhang H, Xu X, Wang X. Numerical analysis and surrogate model optimization of air-cooled battery modules using double-layer heat spreading plates. *Int J Heat Mass Transf* 2021;176:121380. [\[CrossRef\]](#)
- [32] Quanhong L, Caili F. Application of response surface methodology for extraction optimization of germinant pumpkin seeds protein. *Food Chem* 2005;92:701-706. [\[CrossRef\]](#)
- [33] Tao Y, Zhang Z, Sun DW. Experimental and modeling studies of ultrasound-assisted release of phenolics from oak chips into model wine. *Ultrason Sonochem* 2014;21:1839-1848. [\[CrossRef\]](#)
- [34] Guo Z, Chen F, Yang H, Liu K, Zhang L. Kinetics of protein extraction in reverse micelle. *Int J Food Prop* 2015;18:1707-1718. [\[CrossRef\]](#)
- [35] Leser ME, Luisi PL, Paimieri S. The use of reverse micelles for the simultaneous extraction of oil and proteins from vegetable meal. *Biotechnol Bioeng* 1989;34:1140-1146. [\[CrossRef\]](#)
- [36] Wang Z, Li H, Liang M, Yang L. Glutelin and prolamin, different components of rice protein, exert differently in vitro antioxidant activities. *J Cereal Sci* 2016;72:108-116. [\[CrossRef\]](#)
- [37] Zhao X, Zhu H, Zhang B, Chen J, Ao Q, Wang X. XRD, SEM, and XPS analysis of soybean protein powders obtained through extraction involving reverse micelles. *J Am Oil Chem Soc* 2015;92:975-983. [\[CrossRef\]](#)
- [38] Zhang Y, Yang R, Zhang W, Hu Z, Zhao W. Structural characterization and physicochemical properties of protein extracted from soybean meal assisted by steam flash-explosion with dilute acid soaking. *Food Chem* 2017;219:48-53. [\[CrossRef\]](#)
- [39] Carbonaro M, Nucara A. Secondary structure of food proteins by Fourier transform spectroscopy in the mid-infrared region. *Amino Acids* 2010;38:679-690. [\[CrossRef\]](#)
- [40] Baltacıoğlu H, Bayındırlı A, Severcan F. Secondary structure and conformational change of mushroom polyphenol oxidase during thermosonication treatment by using FTIR spectroscopy. *Food Chem* 2017;214:507-514. [\[CrossRef\]](#)
- [41] Güler G, Vorob'ev MM, Vogel V, Mäntele W. Proteolytically-induced changes of secondary structural protein conformation of bovine serum albumin monitored by Fourier transform infrared (FT-IR) and UV-circular dichroism spectroscopy. *Spectrochim Acta A Mol Biomol Spectrosc* 2016;161:8-18. [\[CrossRef\]](#)
- [42] Zhang L, Pan Z, Shen K, Cai X, Zheng B, Miao S. Influence of ultrasound-assisted alkali treatment on the structural properties and functionalities of rice protein. *J Cereal Sci* 2018;79:204-209. [\[CrossRef\]](#)
- [43] Jayaramudu T, Raghavendra GM, Varaprasad K, Sadiku R, Raju KM. Development of novel biodegradable Au nanocomposite hydrogels based on wheat: For inactivation of bacteria. *Carbohydr Polym* 2013;92:2193-2200. [\[CrossRef\]](#)
- [44] Zhao X, Chen F, Xue W, Lee L. FTIR spectra studies on the secondary structures of 7S and 11S globulins from soybean proteins using AOT reverse micellar extraction. *Food Hydrocol* 2008;22:568-575. [\[CrossRef\]](#)